THREE-DIMENSIONAL EFFECTS IN COMPRESSIBLE OPEN CAVITY FLOWS

Huanxin Lai
School of Engineering Sciences
University of Southampton
Southampton, SO17 1BJ, United Kingdom.
h.lai@soton.ac.uk

Kai H. Luo
School of Engineering Sciences
University of Southampton
Southampton, SO17 1BJ, United Kingdom
k.h.luo@soton.ac.uk

ABSTRACT

Direct numerical simulation (DNS) is carried out to study the compressible flow over a fully three-dimensional open cavity, which has a length-to-depth ratio $L/D = 5$ and width-to-depth ratio $W/D = 1$. The Mach number of the incoming flow is $M = 0.85$, and the Reynolds number based on the cavity depth is $Re_D = 5000$. The unsteady flow dynamics is analyzed, focusing on the cross-stream flow patterns, unlike previous studies. The implication for sound generation in the cross-stream direction is discussed. The DNS database contains Reynolds averaged quantities as well as instantaneous ones, making it valuable for model development and validation.

INTRODUCTION

The study of cavity flow has important academic and engineering values. Cavity flow is rich in flow phenomena such as unsteadiness, flow separation and reattachment, three-dimensionality and flow-acoustics interactions, though the geometry is relatively simple. This makes the cavity flow problem a prototype for fluid dynamics and aeroacoustics studies. In engineering applications, compressible flows over open cavities widely occur in devices such as wheel well and bomb bay of aircraft. The three-dimensional (3D) oscillating high-speed flow coupled with large density and pressure fluctuations may lead to optical pathway deviations and structural fatigue and damage.

Despite the 3D nature of most open cavity flows, previous theoretical, experimental and numerical studies typically used two-dimensional (2D) models. Reviews of these studies were provided by Rockell and Naudascher (1978), Blake and Powell (1986), Grace (2001), Colonius (2001) and Takeda and Shieh (2004). Since Rossiter (1964) proposed the "feedback loop" description of flow oscillation, these studies have revealed the existence of two basic flow regimes depending on the cavity length-to-depth ratio L/D. The open cavity flow happens when $L/D < 8\sim10$ for subsonic the incoming flow, and the closed cavity flow occurs when $L/D > 8\sim10$. In the open cavity mode, the shear layer bridges between the front and rear walls of the cavity; and in the closed mode, the shear layer separates from the cavity leading edge, reattaches to the cavity floor and then separates again before the cavity rear wall. Until recent years, 2D models are still widely employed to study the cavity problem. Rowley et al. (2002) observed the transition of shear layer mode to wake mode when the ratio of cavity length to the inflow boundary layer thickness was increased in their 2D simulation. Gloerfelt et al. (2003) studied the noise radiation by a subsonic cavity flow using simulation and acoustic analogy. Larsson et al. (2004) investigated the low Mach number open cavity flow and acoustics while Kim et al. (2004) studied the cavity flow in scramjet engine. These investigations used 2D DNS. On the other hand, 2D analysis of the cavity problem is also carried out by researchers using large eddy simulations (LES), Reynolds averaged Navier-Stokes (RANS) methods and experimental investigations, such as Rizzetta and Visbal (2003), Larcheveque et al. (2003), Gloerfelt et al (2003), Zhang et al (1999), Ashcroft et al. (2003), Strang and Fernando (2004), Unalmis et al. (2004), Kegerise and Spina (2004) and Ashcroft and Zhang (2005). These studies treat a cavity as 2D or 3D without the side walls. Only very recently, numerical investigations of flows in fully 3D cavities were reported (Larcheveque et al., 2004; Gloerfelt, 2004; Larcheveque et al., 2003; Mendonca et al 2003; Avital, 2001; Lai and Luo, 2004). As reviewed by Takeda and Shieh (2004), the 3D effects can reduce the fluctuations in the cavity and will act to suppress the appearance of wake mode or at least to change its parameter dependency. The three-dimensionality also has effects on cavity acoustics. The LES of cavities with different spanwise size (Gloerfelt et al, 2002) shows that the dominate frequencies for a narrower cavity are the first and fourth Rossiter modes, but for a wider cavity the dominancy is changed to the third Rossiter mode. Meanwhile,

Gloerfelt et al (2002) also showed that the reduction of cavity width lowered the sound pressure level (SPL) over the entire spectrum by up to 15 dB because the spanwise coherence of the feedback instabilities was also lowered in the narrower cavity. Indeed, the 3D effects in the cavity flow and acoustics are very important and should be carefully studied. Larcheveque et al (2004) studied the flow in a 3D cavity using LES, but the analysis was focused on the shear layers near the cavity leading edge and vortical structures inside the cavity were not provided.

In this paper we report a DNS of 3D compressible flow in a realistic open cavity configuration. DNS has the advantages of resolving all the scales of fluid motion so that the solution is not influenced by any empirical turbulence model. It provides complete information about a given flow, which is invaluable for understanding flow physics and assessing turbulence models. In the following sections, we first give a brief introduction to the simulation details. The averaged velocity distributions are then presented, followed by detailed analysis of the 3D unsteady flow structures in and around the cavity.

NUMERICAL SIMULATION

Problem Description

The configuration studied in this paper is the cavity used in the wind-tunnel test at the DSTL. The experimental data provided by the DSTL contain time history of pressure signals at a series of sensors. The case studied here is M219, which has no bay door nor instrument installed. The cavity depth is $D = 4$ inches, length $L = 20$ inches and width $W = 4$ inches. So the cavity aspect ratios are $L/D = 5$ and $W/D = 1$. The free-stream Mach number is $M = 0.85$. The Reynolds number based on the depth of the cavity is $Re_D = 1.35\times10^6$ and the boundary layer thickness is around 10.5 mm in the experiments. Because of the limitation of computing resources, we use a lower Reynolds number at $Re_D = 5\times10^3$ in the DNS.

Computational Domain and Grids

The computational domain is decomposed into the cavity block (BL1) and the block outside cavity (BL2), as shown in figure 1. Both the upstream and downstream boundaries are located at $4D$ away from the leading and trailing edges of the cavity, respectively, and the upper horizontal boundary is set at $H = 4D$ so that the computational domain includes a portion of the acoustic near field. The spanwise size of BL2 is set as $W_2=2W$.

The grid points in the two blocks in x-y-z directions are 221×120×101 (BL1) and 401×221×201 (BL2), respectively, with grid points concentrated in the wall layers. An illustration of the grid distribution is shown in figure 1.

Numerical Methods

The full compressible Navier-Stokes equations can be written in a compact notation as following:

$$\frac{\partial U}{\partial t}+\frac{\partial F^I}{\partial x}+\frac{\partial G^I}{\partial y}+\frac{\partial H^I}{\partial z}=\frac{\partial F^V}{\partial x}+\frac{\partial G^V}{\partial y}+\frac{\partial H^V}{\partial z} \qquad (1)$$

where the conservative variables are $U=(\rho,\ \rho u_i,\ E_T)^T$; F^I, G^I, H^I and F^V, G^V, H^V are convective and diffusive fluxes, respectively. The equations are non-dimensionalised. The reference quantities are the cavity depth D, the inflow velocity U_{in}, time scale D/U_{in}, and the density, viscosity, temperature, and the dynamic pressure of the free stream.

The governing equations are discretised in space with a fourth-order central finite difference scheme, and marched in time explicitly with a third-order Runge-Kutta method. Centred schemes are well-suited for DNS because of their low intrinsic numerical dissipation. However, low numerical dissipation may lead to numerical instabilities, especially when shocks are present. Therefore, an entropy splitting method is employed to enable stable numerical solutions at a wide range of the Mach number. The idea of the method is to split the Euler terms into a conservative part and a symmetric part based on an entropy variable, and separate treatments are applied to the two parts. Extensive tests have shown that such a splitting procedure improves the nonlinear stability while minimizing numerical dissipation for both smooth flows and for flows with complex shock-turbulence interactions. In the meantime, a stable high-order numerical boundary treatment is used, based on the summation by part (SBP) approach of Carpenter et al. (1999). With these techniques, high-order and stable results can be obtained. More details of the numerical schemes can be found in Sandham et al. (2002) and Yee et al. (1999).

Boundary Conditions

At the inflow boundary, the mean value of velocity is specified using a $(1/7)^{th}$ power law; density and temperature are specified according to the Crocoo-Busemann temperature-velocity relation. A small disturbance with a magnitude of up to 4% of the mean streamwise velocity is added at the inflow boundary. Meanwhile, the outgoing characteristics are explicitly calculated and allowed to move out of the computational domain.

At the outflow and the upper boundaries, Thompson's (1987, 1990) non-reflecting characteristic boundary conditions are applied, which allow all outgoing waves to propagate smoothly out of the computational domain while keeping incoming waves out. All solid walls including the cavity side walls are assumed to be isothermal and the no-slip boundary condition is imposed.

Parallel Computing

The simulation is carried out using the SBLI (Shock/Boundary-Layer Interaction) code, which is a highly

efficient multi-block code for massively parallel computers. The numerical methods have been introduced above, The code has been validated for various compressible flow and aeroacoustic problems (Sandham et al, 2002; Hu et al, 2003; Sandham et al., 2003).

The present simulation was run with 128 PEs on the UK's HPCx service. The CFL number is set to be 1.0, which corresponds to a non-dimensional time step of 1.0×10^{-4}. The flow enters a self-sustained oscillation state after an initial transient stage of about 15 to 20 non-dimensional time units. Statistical data were collected from about 4 flow-through periods (nondimensional time 52) for a further 5 flow-through periods (64 time units), giving a total of 15,000 samples.

RESULTS

Sound Pressure Level

The experimental data available for comparison are limited. Figure 2 shows the sound pressure level (SPL) at a series of monitoring points on the cavity floor along the line z/D = 0.625. The SPL is defined as follows:

$$SPL(dB) = 20log_{10}\left(p'_{rms}/2\times10^{5}Pa\right) \quad (2)$$

where p' is the root-mean-square of the sound pressure. For comparison, an earlier result of a DNS at M=0.85 and Re_D = 1×10^3 (Lai and Luo, 2004) is also shown in figure 2. It seems that the Reynolds number effects are large in the low Reynolds number range. At Re_D = 5×10^3, the DNS data agree with the experimental data very well. It remains to be tested whether or not a higher Reynolds number simulation would produce different results.

Mean Flow

The time-averaged velocity profiles of the cavity are shown in figure 3. Figure 3a is the distribution of streamwise velocity U in the central plane. At the cavity entrance, the velocity profile changes from a boundary layer to a (free) shear layer. After impinging on the rear wall, the flow is partly deflected towards to the cavity floor and forms a reverse-flow wall layer. The mean flow exiting the cavity seems to be attached to the cavity plate downstream, although separated flow is seen in the instantaneous velocity field. Flow recirculation inside the cavity is confirmed by comparing the distributions of U at y=0.95D in figure 3c, where U along the spanwise direction is generally positive and that at y=0.5D in figure 3d, where U is mostly negative. The spanwise variation of V at y=0.5D (figure 3e) indicates the existence of the streamwise vortices inside the cavity. In figure 3f, the U distribution just above the cavity at y =1.1D shows strong influence of the cavity.

3D Flow Structures

Figure 4 shows a series of top views of the vortical structures defined by the iso-surface of the Q criterion (Hunt et al., 1988):

$$Q = \frac{1}{2}\left(\Omega_{ij} - S_{ij}\right) = -\frac{1}{2}\frac{\partial u_i}{\partial x_j}\frac{\partial u_j}{\partial x_i} > 0 \quad (4)$$

where S_{ij} and Ω_{ij} are the symmetric and antisymmetric components of the gradient of velocity vector. So the Q criterion is the second invariant of the velocity gradient. The region enclosed by an iso-surface of a positive Q value defines a tube of vortex. Shown in figure 4 is the vortical structures deduced using the iso-surface Q=20$(U_{in}/L)^2$ (Larcheveque et al., 2003). Quite complex and unsteady vortex structures are featured. Large spanwise vortices are generated periodically near the cavity leading edge, due to the Kelvin-Helmholtz instabilities. These vortices are spanwise rollers only at the very beginning but quickly become Lambda-like vortices. The zone where 2D vortical structures dominate is much short than seen in 2D simulations. Shortly afterwards, the large vortices break up into smaller vortices, which are irregular and highly three-dimensional. The vertical structures are especially complex near the cavity rear wall, due to flow impingement and recirculation. However, in the region downstream of the cavity trailing edge, the vortices become aligned mostly in the streamwise direction, similar to the streaks found in boundary layers. A 3D view of the vortical structures shown in figure 5 confirms the above observations but further reveals the vortical structures in the recirculation zone due to flow deflection by the rear wall.

Figure 6 shows the distributions of the streamwise velocity and the cross-stream velocity vectors in planes normal to the streamwise direction. Six plane cuts at x/D= 0.5, 1.5, 2.5, 3.5, 4.5 and 5.2, denoted by CUT1~ CUT6 respectively, are plotted for three instants. The predominant feature in all the plots is that the instantaneous flow is quite non-symmetric about the central plane, although the mean velocities are symmetric as shown in figure 3. In CUT1, the flow is nearly 2D and the streamwise velocity u is positive. 3D structures start to appear in CUT2 and become the dominant feature from CUT3 onwards. The streamwise vortices are typically smaller than or about the size of 0.5D. Their time scales are also short, compared with the period of the second Rossiter mode. However, they provide the mechanism for the mass and momentum exchange between the cavity and the surrounding in the cross-stream direction, which is lacking in any 2D model. It would be interesting to conduct further analysis to examine how such 3D features would affect the pressure field and sound generation, and consequently the performance of any mounted instrument in the cavity. Finally, it is noticed that negative streamwise velocity exists in CUT6. This indicates that flow may reverse from downstream of the cavity trailing edge into the cavity at various instants.

SUMMARY

DNS of compressible flow over a fully 3D open cavity was conducted using a highly efficient parallelized code. An accurate database was obtained, which would be used for validating and constructing subgrid-scale models for LES. As previous studies had concentrated on spanwise vortical structures and acoustic feedback in the streamwise direction, the present paper focused on the analysis of the flow structures in the cross-stream directions. It was observed that at a Reynolds number 5000, the cavity flow lost symmetry in the spanwise direction in the instantaneous sense. Non-symmetric vortices caused flow exchange between the cavity and the surrounding in the cross-stream directions. These vortices had smaller time and length scales than those associated with the first few Rossiter modes, but they could have important implications for pressure fluctuations in the cross-stream directions and consequently the performance of instrument installed in the cavity. Further investigation is needed to clarify this issue.

ACKNOWLEDGEMENTS

The work was funded by the UK EPSRC and MOD/DSTL under Grant No. GR/R85303/01. Thanks are due to Dr. Trevor Birch, the project manager at DSTL and Dr. Graham Foster who supplied the experimental data. The computing resources were from the UK Turbulence Consortium under the EPSRC Grant No. GR/R64964/01.

REFERENCES

Ashcroft, G. B., Takeda, K. and Zhang, X., 2003, "A Numerical Investigation of Noise Radiated by a Turbulent Flow over a Cavity", *Journal of Sound and Vibration*, Vol.265, pp.43-60.

Ashcroft, G. and Zhang, X., 2005, "Vortical Structures over Rectangular Cavities at Low Speed," *Physics of Fluids*, Vol.17, No. 1, pp. 1-8.

Avital, E. J., 2001, "Direct and Large Eddy Simulations of Compressible Open Cavity Flows," in *Direct and Large-Eddy Simulation IV*, Edited by B. J. Geuts, R. Friedrich and O. Metals, Kluwer Academic Publishers, Dordrecht/Boston/London, pp. 213-220.

Blake, W. K., and Powell, A., 1986, "The development of contemporary views of flow-tone generation". In *Recent Advances in Aeroacoustics*, Springer., pp.247-345.

Carpenter, M. H., Nordstrom, J., and Gottlieb, D., 1999, "A stable and conservative interface treatment of arbitrary spatial accuracy", *Journal of Computational Physics,* Vol. 148, No. 2, pp. 341–365.

Colonius, T., 2001, "An overview of simulation, modeling, and active control of flow/acoustic resonance in open cavities", *AIAA Paper* 2001-0076.

Gloerfelt, X., 2004, "Large-eddy simulation of a high Reynolds number flow over a cavity including radiated noise", *AIAA Paper* 2004-2863.

Gloerfelt, X., Bailly, C., and Juve, D., 2003, "Direct computation of the noise radiated by a subsonic cavity flow and application of integral methods", *Journal of Sound and Vibration*, Vol. 266, pp. 119-146.

Gloerfelt, X., Bogey, C., and Bailly, C., 2002, "LES of noise radiated by a flow over a rectangular cavity", *International workshop on "LES for Acoustics"*, 7.-8. October 2002, DLR Gottingen, Germany.

Grace, S., 2001, "An Overview of Computational Aeroacoustic Techniques Applied to Cavity Noise Prediction", *AIAA Paper* 2001-0510.

Hu, Z. W., Morfey, C. L., and Sandham, N. D., 2003, "Large Eddy Simulation of Plane Jet Sound Radiation", *AIAA Paper* 2003-3166.

Hunt, J. C. R., Wray, A. A., and Moin, P., 1988, "Eddies, stream, and convergence zones in turbulent flows", In *Proceedings of the 1988 Summer Program* (Center for Turbulence Research, Stanford, CA), pp. 193–208.

Kegerise, M. A., and Spina, E. F., 2004, "Mode-Switching and Nonlinear Effects in Compressible Flow over a Cavity," *Physics of Fluids*, Vol. 16, No. 3, pp. 678-687.

Kim, C., Yu, S., and Zhang, Z., 2004, "Cavity Flow in Scramjet Engine by Space-Time Conservation and Solution Element Method", *AIAA Journal*, Vol.42, No.5, pp. 912-919.

Lai, H and Luo, K.H., 2004, "Direct Numerical Simulation of Three-Dimensional Compressible Flows in an Open Cavity", in *Recent Advances in Fluid Mechanics* (Proceedings of the Fourth International Conference on Fluid Mechanics), edited by F Zhuang and J Li, Tsinghua University Press and Springer, PP. 790-793.

Larcheveque, L., Sagaut, P., Mary, I., and Labbe, O., 2003, "Large-eddy simulation of a compressible flow past a deep cavity", *Physics of Fluids*, Vol. 15, No. 1, pp. 193~210.

Larcheveque, L., Sagaut, P., Le, T. and Comte, P., 2004, "Large-Eddy Simulation of a Compressible Flow in a Three-Dimensional Open Cavity at High Reynolds Number," *Journal of Fluid Mechanics*, Vol. 516, pp.265-301.

Larsson, J., Davidson, L., Olsson, M., and Erikson, L., 2004, "Aeroacoustic Investigation of an Open Cavity at Low Mach Number", *AIAA Journal*, Vol.12, No.12, pp. 2462-2473.

Lin, J.C., and Rockwell, D., 2001, "Organized Oscillations of Initially Turbulent Flow Past a Cavity", AIAA Journal, Vol.39, No.6, pp. 1139-1151.

Mendonca, F., Allen, R., Charentenay, J. and Kirkham, D., 2003, "CFD Prediction of Narrowband and Broadband Cavity Acoustics at M=0.85," *AIAA Paper* 2003-3303.

Rizzetta, D., and Visbal, M. R., 2003, "Large-eddy Simulation of Supersonic Cavity Flow Fields including Flow Control", *AIAA Journal*, Vol. 41, No. 8, pp. 1452-1462.

Rockwell, D., and Naudascher, E., 1978, "Review- Self-sustaining oscillations of flow past cavities", *ASME Journal of Fluids Engineering*, Vol. 100, No.2, pp. 152-165.

Rossiter, J. E., 1964, "Wind tunnel experiments on the flow over rectangular cavities at subsonic and transonic speeds", *Ministry of Aviation, Aeronautical Research Council, R&M* 3438.

Rowley, C. W., Colonius, T., and Basu, A. J., 2002, "On self-sustained oscillations in two-dimensional compressible flow over rectangular cavities", *Journal of Fluid Mechanics*, Vol. 455, pp. 315-346.

Sandham, N.D., Li, Q., and Yee, H.C., 2002, "Entropy splitting for high order numerical simulation of compressible turbulence", *Journal of Computational Physics*, Vol. 178, No. 2, pp. 307–322.

Sandham, N. D., Yao, Y. F., and Lawal, A. A., 2003, "Large-eddy simulation of transonic turbulent flow over a bump", *International Journal of Heat and Fluid Flow*, Vol.24, pp. 584~595

Strang, E., and Fernando, H. J. S., 2004, "Shear-Induced Mixing and Transport from a Rectangular Cavity," *Journal of Fluid Mechanics*, Vol.520, pp.23-49.

Takeda, K., and Shieh, C. M., 2004, "Cavity Tones by Computational Aeroacoustics", *International Journal of Computational Fluid Dynamics*, Vol. 18, No.6, pp.439-454.

Thompson, K. W., 1987, "Time dependent boundary conditions for hyperbolic systems", *Journal of computational physics*, Vol. 68, pp. 1-24.

Thompson, K. W., 1990, "Time dependent boundary conditions for hyperbolic systems, II", *Journal of computational physics*, Vol. 89, pp. 439-461.

Unalmis, O. H., Clemens, N. T., and Dolling, D. S., 2004, "Cavity Oscillation Mechanisms in High-Speed Flows", *AIAA Journal*, Vol. 42, No.10, pp.2035-2041.

Yee, H.C., Sandham, N.D., and Djomehri, M.J., 1999, "Low-dissipative high-order shock-capturing methods using characteristic-based filters", *Journal of Computational Physics*, Vol. 150, pp. 199–238.

Zhang, X., Chen, X. X., Rona, A., and Edward, J. A., 1999, "Attenuation of Cavity Flow Oscillation through Leading Edge Flow Control", *Journal of Sound and Vibration*, Vol.221, No.1, pp.23-47.

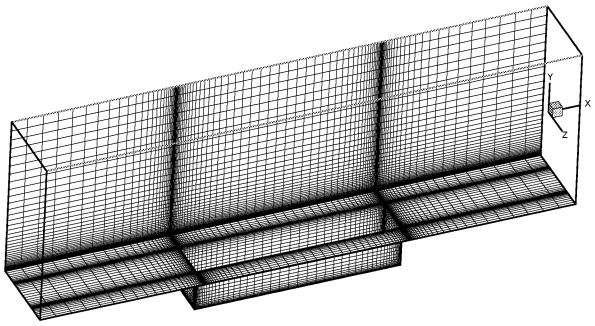

Figure 1 The multi-block computational domain and grids.

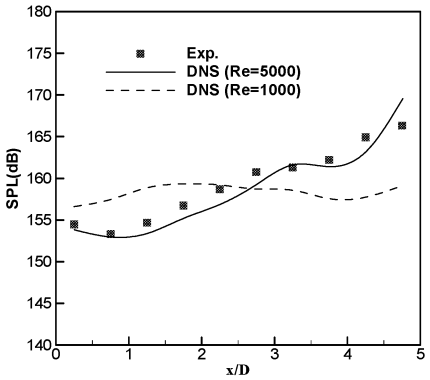

Figure 2 Comparison of SPL along the cavity floor.

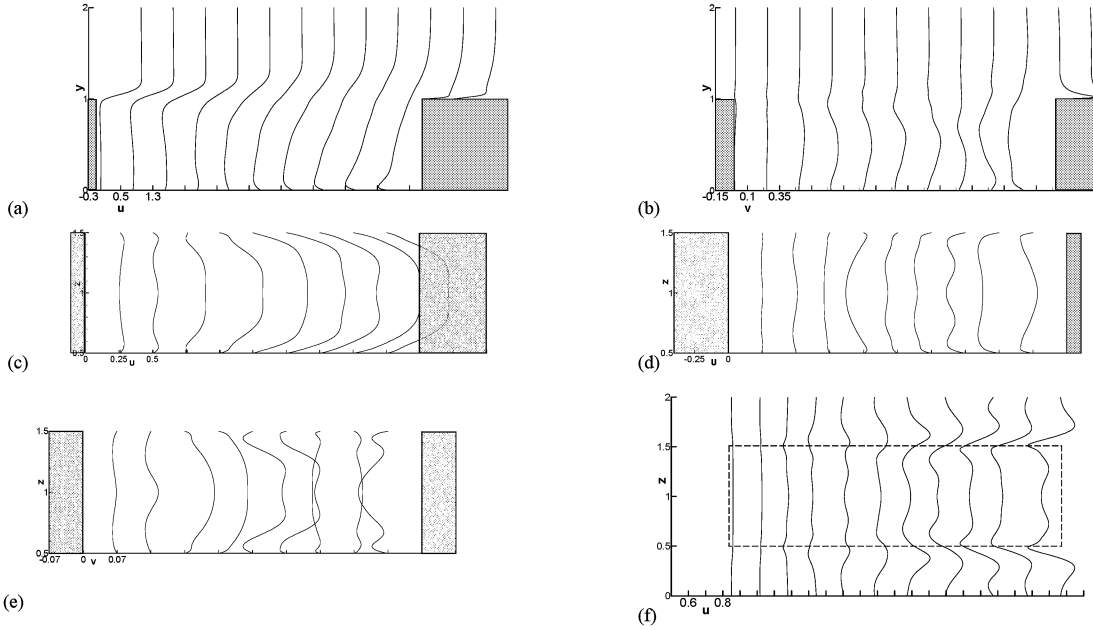

Figure 3. Mean velocity profiles. (a) U in the central plane, from left to right x/D= 0.25, 0.75, 1.25, 1.75,2.25, 2.75, 3.25, 3.75, 4.25, 4.75, 5, 5.25; (b) V in the central plane, x/D same with (a); (c) U at y/D=0.95, x/D=0.5, 1, 1.5, 2, 2.5, 3, 3.5, 4, 4.5; (d) U at y/D=0.5, x/D same with (c); (e). V at y/D=0.5, x/D same as (c); (f) U at y/D=1.1, x/D same with (c).

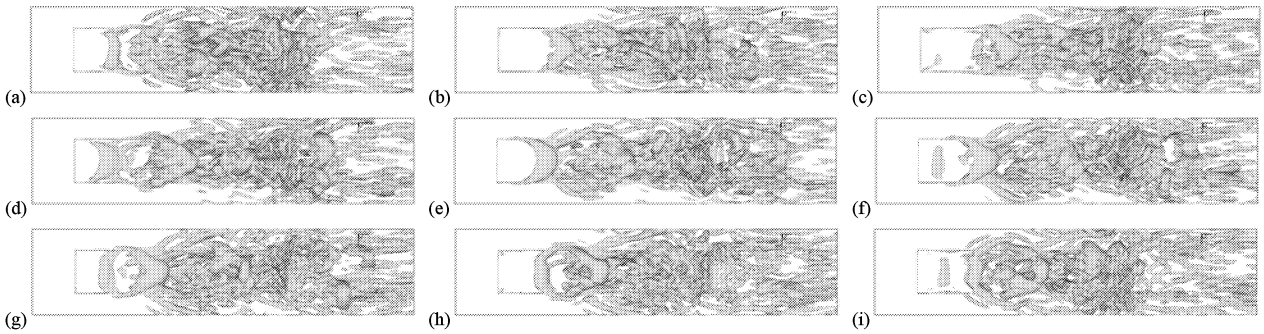

Figure 4 Snapshots of the Q criterion at nine instants during a period associated with the second Rossiter mode.

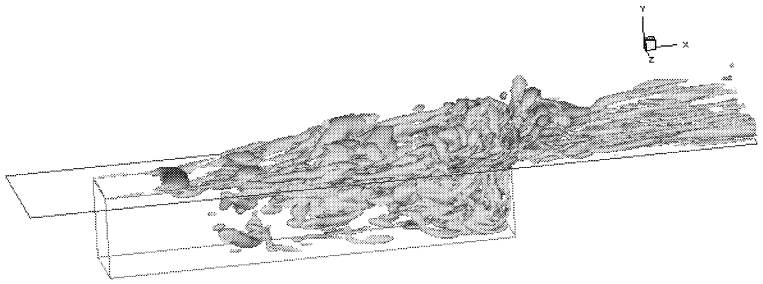

Figure 5 A representative image of 3D vortical structures defined by the *Q* criterion..

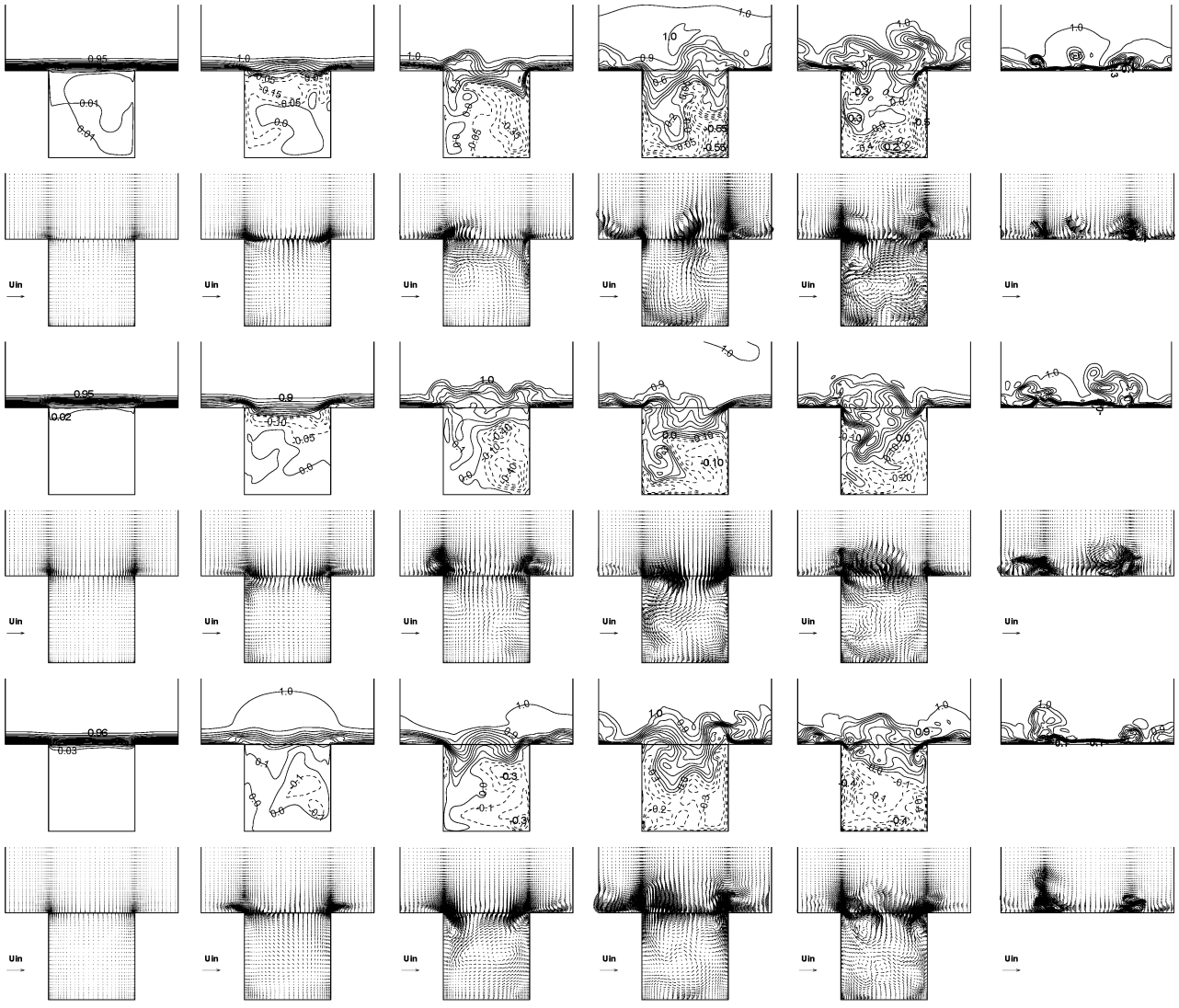

Figure 6 Distributions of streamwise velocity and cross-stream velocity vectors at *t* (rows 1 and 2), t+1/3T2 (rows 3 and 4) and t+2/3T2 (rows 5 and 6). T2 is the period corresponding to the second Rossiter mode. Columns 1~6 from left to right correspond to CUT1~CUT6 (*x/D*= 0.5, 1.5, 2.5, 3.5, 4.5 and 5.2), respectively.